High-Q Narrowband Tunable Combline Bandpass Filters Using MEMS Capacitor Banks and Piezomotors

Siamak Fouladi, *Member, IEEE*, Fengxi Huang, *Student Member, IEEE*, Winter Dong Yan, *Member, IEEE*, and Raafat R. Mansour, *Fellow, IEEE*

***Abstract*—This paper presents the design and implementation of a new class of evanescent tunable combline bandpass filters based on electronic tuning with the use of RF microelectromechanical systems (RF-MEMS) capacitor banks and also mechanical tuning using piezomotors. The use of microelectromechanical systems tuning circuit results in compact implementation of the proposed filters with high-Q and near to zero dc power consumption. The proposed filter structures consist of combline resonators with tuning disks that are either mechanically moveable using piezomotors or are loaded with RF-MEMS capacitor banks. Two- and six-pole tunable bandpass filters are designed and measured based on the proposed tuning concept. The two-pole tunable filter operates at 2.5 GHz with a bandwidth of 22 MHz and demonstrates a tuning range of 110 MHz, while the quality factor is better than 374 (1300–374 over the tuning range). The six-pole tunable filter with RF-MEMS capacitor banks operates from 2.634 to 2.59 GHz (44-MHz tuning range). The proposed tunable filter structures can also be implemented using alternative technologies such as barium–strontium–titanate varactors.**

***Index Terms*—Combline filter, tunable filters, high Q, electronic tuning, mechanical tuning, RF microelectromechanical systems (RF-MEMS), piezomotor.**

I. Introduction

As WIRELESS devices become more and more compact, the development of inexpensive and miniaturized tunable filters with a superior performance is crucial not only for mobile handheld devices, but also to wireless infrastructure equipment. It can benefit from tunable filter technologies in three different areas; first, installing wireless infrastructure equipment, such as a remote radio unit (RRU) on top of a 15-story high communication tower, is a very costly job. By using tunable filters, one installation can serve many years since if there is a need to change the frequency or bandwidth, it can be done through remote electronic tuning, rather than installing a new filter. Secondly, in urban areas, there is very limited space for wireless service providers to install their base stations due to expensive real estates and/or maximum weight loading constrains on certain installation locations such as light poles or power lines. Therefore, once an installation site is acquired, it is natural for wireless service providers to stuff as many functions, such as multistandards and multibands, into one site as possible. A tunable filter is a key element to enable such possibility. Finally, the frequency spectrum is a very limited and expensive resource. To construct a wireless network that covers large geographic locations, it is not quite unusual for one wireless service provider to use a different frequency spectrum and bandwidth at different locations, even within one single network. This complex frequency spectrum allocation will require many different fixed filters to be built. However, by using tunable filters, it is quite possible to just use one type of filter to construct the whole network.

Various tuning techniques have been developed to construct tunable filters. Mechanical tuning [1], [2] magnetic tuning [3], and electrical tuning [4], [5] are the most common. In terms of quality factor, power-handling capability, and linearity, mechanical tuning is superior to the other two tuning techniques. Unfortunately, due to their bulky size, heavy weight, and low tuning speed, mechanically tunable filters have limited applications. Microelectromechanical systems (MEMS) technology has the potential to produce highly miniaturized tunable filters [6]–[13]. Planar tunable filters employing MEMS devices are reported in [6]–[8]. These filters cover a frequency range from 1 to 6 GHz with filter Q values between 85–250. Since the RF microelectromechanical systems (RF-MEMS) devices have very low insertion loss, Q of these planar filters are limited by the resonator Q. In addition to a relatively low quality factor, they require complicated MEMS fabrication for monolithic integration of MEMS devices with filters. A variety of nonplanar tunable filters using RF-MEMS technology have been reported in [9]–[11]. The evanescent-mode cavity filter in [9] utilizes capacitive RF-MEMS switch networks and operates from 4.07 to 5.58 GHz with a Q from 300 to 500. Tunable dielectric resonator filters using RF-MEMS devices with exceptional Q values above 500, over the entire tuning range, are reported in [10]. Although these filters have higher Q values compared to the planar tunable filters, they still require complicated RF-MEMS fabrication and assembly of the tuning elements inside the cavities. Tunable filters using substrate integrated waveguide (SIW) technology and off-the-shelf RF-MEMS

Manuscript received July 11, 2012; revised October 02, 2012; accepted October 15, 2012. Date of publication December 04, 2012; date of current version January 17, 2013. This paper is an expanded paper from the IEEE MTT-S International Microwave Symposium, Montreal, QC, Canada, June 17–22, 2012.

S. Fouladi is with the Wireless Semiconductor Division, Avago Technologies, San Jose, CA 95131 USA (e-mail: siamak.fouladi@avagotech.com).

F. Huang and R. R. Mansour are with the Department of Electrical and Computer Engineering, University of Waterloo, Waterloo, ON, Canada N2L 3G1 (e-mail: fxhuang@uwaterloo.ca; rmansour@uwaterloo.ca).

W. D. Yan is with the Research and Development Center, Huawei Technologies, Kanata, Canada K2K 3J1 (e-mail: winter.yan@huawei.com).

Color versions of one or more of the figures in this paper are available online at http://ieeexplore.ieee.org.

Digital Object Identifier 10.1109/TMTT.2012.2226601

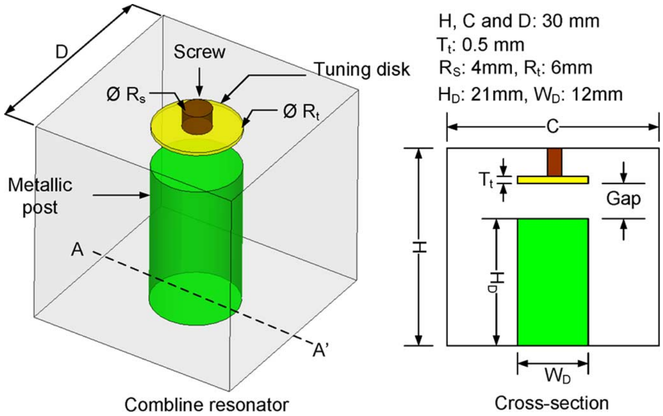

Fig. 1. Combline tunable resonator with tuning disk.

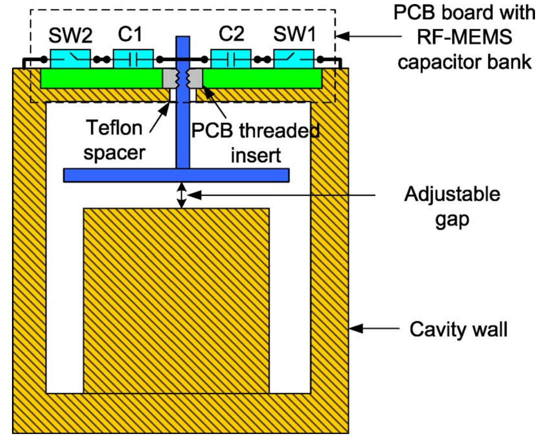

Fig. 2. Schematic drawing of the proposed tunable resonator.

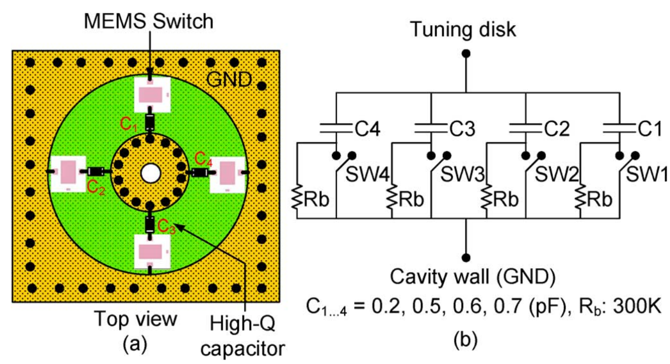

Fig. 3. (a) Schematic diagram of the RF-MEMS tuning circuit and (b) the circuit model.

switches are presented in [12] and [13]. The two-pole filter in [13] operates from 1.2 to 1.6 GHz with Q values from 93 to 132 over the tuning range. A novel tuning approach of combline evanescent-mode cavity filters using commercially available RF-MEMS switches is reported by the authors in [14]. A two-pole tunable bandpass filter is demonstrated that achieves a high-Q above 374 over the entire tuning range from 2.503 to 2.393 GHz (110-MHz tuning). In this paper, the concept is thoroughly analyzed and we also expand the proposed tuning concept to higher order combline filters with more stringent requirements for multiband wireless applications. For the first time, we present six-pole tunable filters using both RF-MEMS tuning circuits and piezomotors with superior performance in terms of Q values.

II. Proposed Tuning Concept

Fig. 1 shows the 3-D view and cross-sectional view of a conventional combline resonator. The resonator can be tuned by adjusting the gap between the metallic post and tuning disk. This can be achieved by manual tuning using a screw or by automatic tuning using a driving mechanism such as motors. The use of conventional mechanical tuning using stepper motors can result in fine tuning steps, high-power handling, and high Q; however, these motors are usually very expensive and bulky, increasing the total weight and size of the tunable filter. In this paper, we are proposing the use of inexpensive tuning mechanisms based on RF-MEMS switched capacitor banks and piezomotors.

Fig. 2 demonstrates the structure of the proposed tunable resonator based on RF-MEMS switched capacitor banks. As shown in this figure, the tuning disk is isolated from the cavity wall with a Teflon spacer. An RF-MEMS capacitor bank is implemented on a printed circuit board (PCB) and is assembled on top of the cavity. The tuning disk is connected to the PCB board through a threaded insert on the PCB board. The variable loading effect of the capacitor bank on the tuning disk is used to tune the resonator. A simplified schematic view and the equivalent circuit diagram of the RF-MEMS tuning circuit is presented in Fig. 3. The switched capacitor bank consists of high-Q capacitors in series with RF-MEMS contact type switches. By turning the MEMS switches on and off, using a dc actuation voltage, it is possible to change the value of the capacitor bank and adjust the resonant frequency of the cavity. The use of RF-MEMS switched capacitor bank results in improved performance in terms of Q, insertion loss, power handling, and linearity for the proposed tunable filter.

III. Tunable Resonator

A tunable resonator is designed using the proposed structure and the tuning circuit shown in Fig. 3. The capacitor bank consists of four high-Q capacitors C_1–C_4 in series with four RF-MEMS switches. Each one of the MEMS switches has a separate bias voltage and can be actuated separately. Using this circuit, the resonator can be tuned to 16 different states based on the value of the capacitor bank. Fig. 5 shows the simulated resonance frequency of a single resonator for different values of the capacitor bank when $C_1 = 0.2$ pF, $C_2 = 0.5$ pF, $C_3 = 0.6$ pF, and $C_4 = 0.7$ pF. As seen in this figure, a tuning range of 168 MHz from 2.5 to 2.332 GHz is achieved.

A photograph of the assembled tunable resonator is shown in Fig. 4(a). The resonator was machined from copper and inside the cavity was sputtered with silver for a higher Q value. The tuning circuit was mounted on top of the lid and glued with silver epoxy. Fig. 4(b) shows the RF-MEMS capacitor bank. High-Q ($Q > 150$ at 2.5 GHz) multilayer ceramic capacitors from Johanson Technology (S-series) and Radant single-pole single-throw (SPST) RF-MEMS switches (RMSW101) are mounted on a Rogers RO4350 PCB board. Each MEMS swicth is actuated separately with an actuation voltage of 90 V and zero dc current (near to zero dc power consumption). The total size

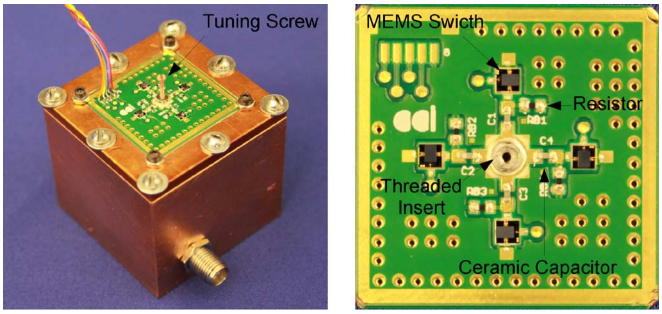

(a) (b)

Fig. 4. (a) Proposed tunable resonator. (b) RF-MEMS switched capacitor bank.

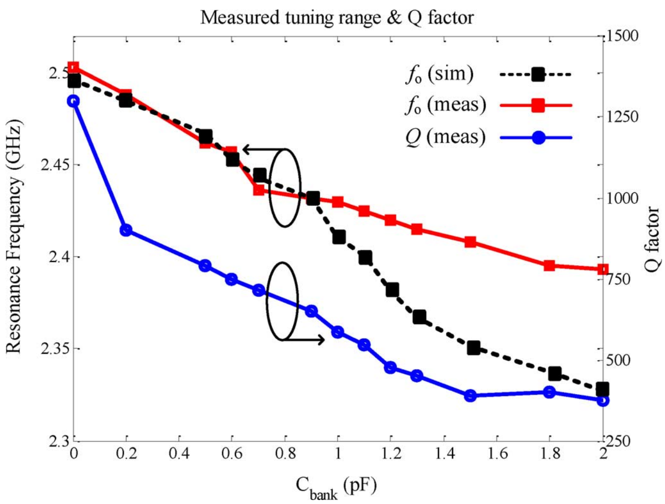

Fig. 5. Simulated and measured resonance frequency and Q versus capacitance value for single resonator.

of the PCB for each capacitor bank is 2.5 cm × 2.5 cm. The measured tuning response and Q of the tunable resonator is presented in Fig. 5. The resonator is tuned from 2.503 to 2.393 GHz (110 MHz), while the measured Q is from 1301 to 374 for all the tuning range.

IV. Two-Pole Tunable Bandpass Filter

Employing the constructed tunable resonator, a two-pole tunable bandpass filter is designed and simulated using HFSS. Fig. 6 shows the full-wave simulation model of the filter. For electromagnetic (EM) simulations, the MEMS tuning circuits are included in the model. A Q factor of 150 at 2.5 GHz is assumed for the fixed ceramic capacitors. The MEMS switch is modeled with a small series capacitor and resistor for the "off" and "on" states, respectively ($C_{\mathrm{off}} = 80$ fF and $R_{\mathrm{on}} = 0.5\ \Omega$). Fig. 7 shows the simulated S-parameters of the designed tunable bandpass filter for three (three out of 16) different tuning states. Simulation results demonstrate that the filter operates at 2.5 GHz with a bandwidth of 22 MHz (0.9%) and a return loss better than 20 dB. It exhibits an insertion loss of 0.44 dB for the first state, when all the switches are "off" and the capacitive loading on the tuning disk is almost zero. The center frequency can be tuned to different states from 2.5 to 2.345 GHz, while the bandwidth varies from 20 to 22 MHz and the return loss is better than 12 dB.

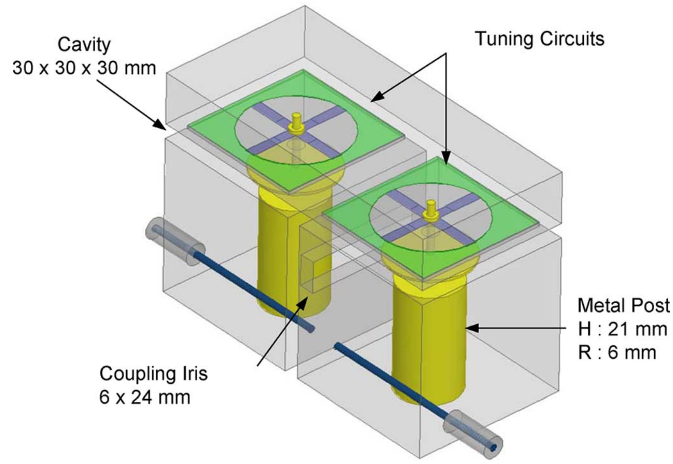

Fig. 6. 3-D EM model of the two-pole tunable filter.

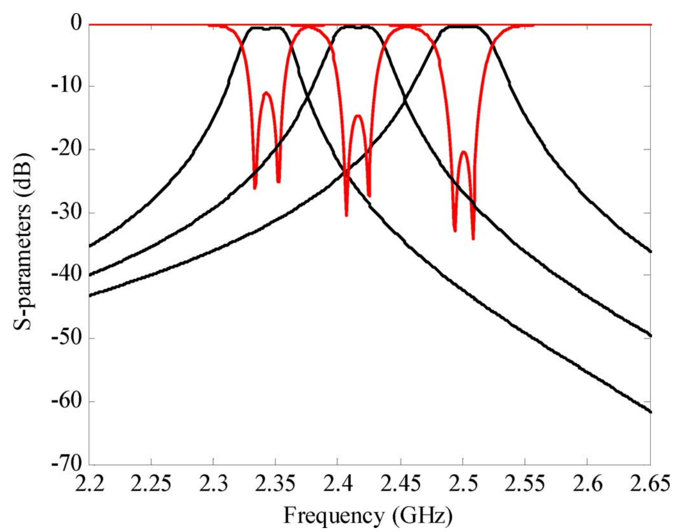

Fig. 7. Simulated S-parameters of the designed filter.

A two-pole tunable combline filter was fabricated and measured. The filter housing was made of aluminum and plated with copper for improved performance. The tuning circuits with RF-MEMS capacitor banks were assembled on top of the lid, as shown in Fig. 8. There are screws connected to the tuning disks. These screws are used only for the initial tuning of the filter after assembly. There are biasing wires for each one of the capacitor banks and each set of MEMS switches. The MEMS switches are turned on and off in a way that the two capacitor banks have the same capacitance values and the two resonators are tuned synchronously. Measurement results for the two-pole tunable bandpass filter are presented in Fig. 9. As shown in this figure, for the first state, the filter operates at 2.5 GHz with a 23-MHz bandwidth and 1.32-dB insertion loss. A maximum tuning range of 110 MHz from 2.503 to 2.393 GHz is achieved using the RF-MEMS tuning circuits. The return loss is better than 14 dB and the insertion loss is less than 2.4 dB for all the tuning states.

The measured return loss when $C_{\mathrm{bank}} = C_3 = 0.6$ pF ($\mathrm{SW}_{1,2,4}$ are "off") shows that the two resonators are not completely tuned to the same frequency. This is due to the small difference in the capacitance values of the two ceramic capacitors

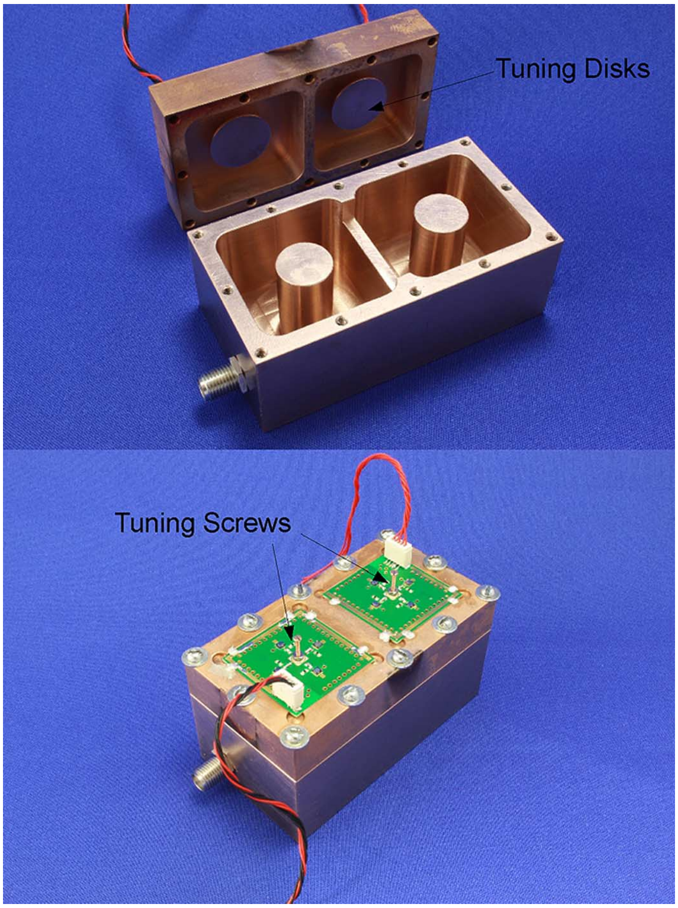

Fig. 8. Assembled two-pole tunable filter with MEMS capacitor bank.

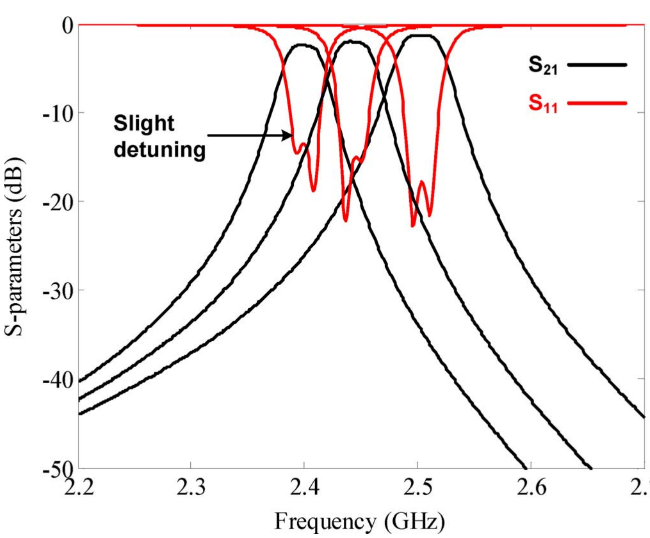

Fig. 9. Measured S-parameters of the two-pole tunable filter.

(C_3), in each capacitor bank, which was not accounted for in the simulations. For this type of discrete tuning, it is necessary for the two capacitor banks to have exactly the same capacitance values. The measurement results validate the simulations and the feasibility of using the proposed tuning approach for combline bandpass filters.

TABLE I
SUMMARY OF SPECIFICATIONS FOR WiMAX TUNABLE BANDPASS FILTER

Item	Frequency Band	Specification
f_c Tunable Range	2565-2635 MHz	70 MHz Tuning
Working Band	2550-2650 MHz	30 MHz Bandwidth
Return Loss	f_c ±15 MHz	≥16dB@P1, ≥18dB@P2
Insertion Loss	f_c ±15 MHz	≤1.8 dB
Rejection	5 MHz offset	≥25 dB

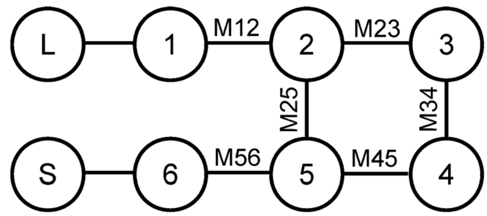

$$M=\begin{pmatrix} 0 & 0.7949 & 0 & 0 & 0 & 0 \\ 0.7949 & 0 & 0.5614 & 0 & -0.1673 & 0 \\ 0 & 0.5614 & 0 & 0.7069 & 0 & 0 \\ 0 & 0 & 0.7069 & 0 & 0.5614 & 0 \\ 0 & -0.1673 & 0 & 0.5614 & 0 & 0.7949 \\ 0 & 0 & 0 & 0 & 0.7949 & 0 \end{pmatrix}$$

Fig. 10. Coupling scheme and matrix of the six-pole tunable filter.

V. WiMAX TUNABLE BANDPASS FILTER

Tight channel spacing requirements for the current wireless standards call for filters with a very sharp frequency roll-off. As channels are packed more closely together, higher order coupled resonator filters are required and for this reason filter specs become more demanding. In this section, we present the design and implementation of a tunable bandpass WiMAX filter operating at 2.5 GHz. Some of the filter requirements are presented in Table I. The sharp frequency roll-off at the band edge (≥25 dB, 5-MHz offset from passband) requires a combline filter with a higher number of cavities. Based on filter synthesis in order to meet the filter requirements, an Elliptic filter with at least six coupled cavities is required. Fig. 10 shows the coupling scheme and the coupling matrix from the filter synthesis using coupling matrix method [15]. Two different implementations of this tunable filter are presented in this paper. The two filters have the same coupled cavity combline structure with two different tuning mechanisms. The first filter is using piezomotors as tuning elements, while the second filter employs RF-MEMS switched capacitor banks.

A. Tunable WiMAX Filter With Piezomotors

The same resonator structure with the dimensions shown in Fig. 1 is used to design the six-pole filter. EM optimization with HFSS is used to find the dimensions of the coupling irises in order to achieve the coupling matrix elements listed in Fig. 10. For positive coupling values, as shown in Fig. 11(a), a rectangular iris with width and height of $W = 6$ mm and $H = 17.2$ mm is used and the parameters L_{ij} are optimized to obtain the different coupling values between resonators. For the negative coupling value between resonators R_2 and R_5, a probe with a length L_p is used, as shown in Fig. 11(b). The location and the length of this probe are optimized in HFSS to achieve

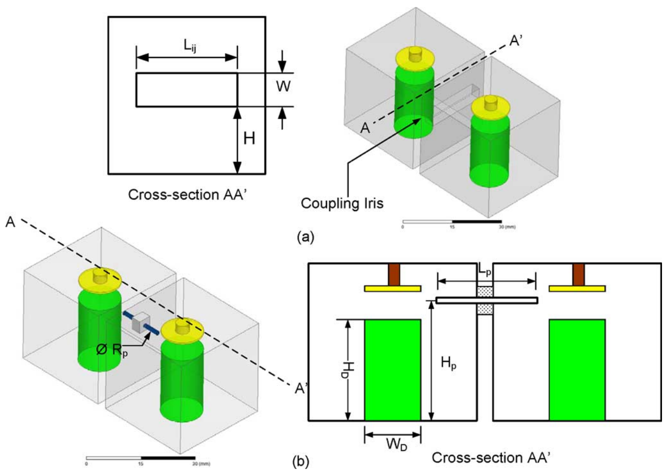

Fig. 11. EM models to find: (a) positive coupling and (b) negative coupling between the combline resonators.

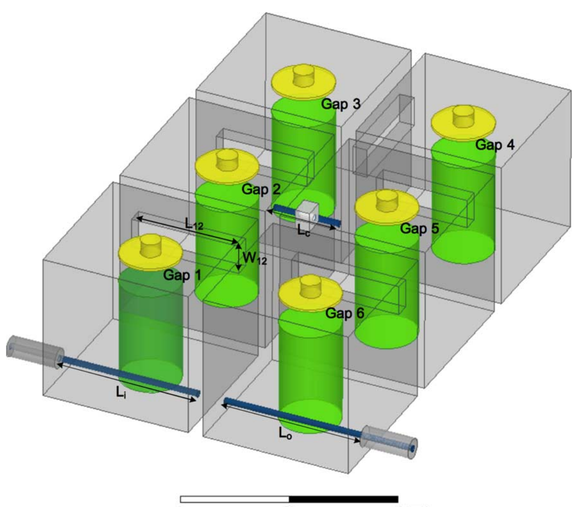

Fig. 12. 3-D EM model of the six-pole tunable filter.

TABLE II
OPTIMIZED DIMENSIONS FOR THE SIX-POLE TUNABLE FILTER

Parameter	Value
Iris Height, Width	H=17.2mm, W=6mm
Positive Coupling Iris Length	$L_{12} = L_{56}$=22.48mm $L_{23} = L_{45}$=19.08mm L_{34}=20.47mm
Negative Coupling Probe Length, Height	L_p=13.4mm, H_p=20.375mm
Input/Output Probe Length, Height	$L_{i,o}$=29.28mm, $H_{i,o}$=4.2mm
Tuning Disk Gap Values at 2.565GHz	G_1=5.29mm, G_2=5.53mm, G_3=5.47mm
Tuning Disk Gap Values at 2.600GHz	G_1=5.71mm, G_2=6.01mm, G_3=5.93mm
Tuning Disk Gap Values at 2.635GHz	G_1=6.22mm, G_2=6.61mm, G_3=6.52mm

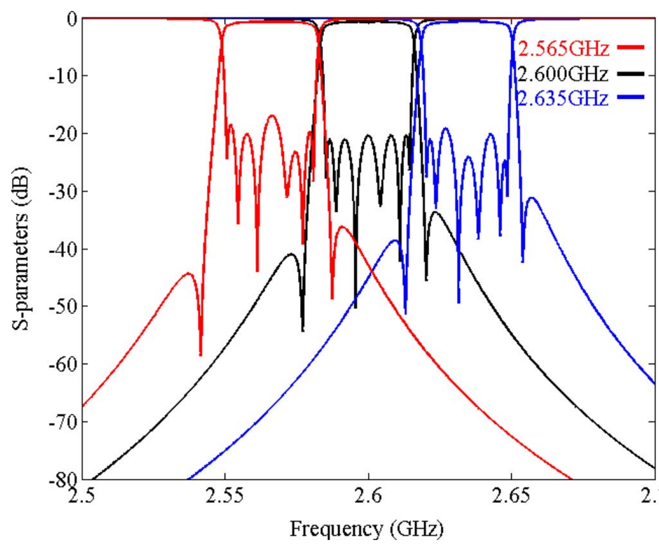

Fig. 13. Simulated S-parameters of the designed six-pole tunable combline filter.

the required coupling value, $M_{25} = -0.1673$. Fig. 12 shows the 3-D EM model of the six-pole tunable filter with geometric dimensions as listed in Table II. Simulated S-parameters for the designed six-pole tunable bandpass filter are presented in Fig. 13 for three different tuning states at $f_1 = 2.635$ GHz, $f_2 = 2.6$ GHz, and $f_3 = 2.565$ GHz. For the tunable filter with piezomotors, tuning is achieved by adjusting the gap value between the tuning disk and the metallic post for each resonator G_i $(i = 1, \ldots, 6)$. The required G_i values for the three tuning states are listed in Table II. Note that due to the symmetric structure of the filter, $G_6 = G_1$, $G_5 = G_2$, and $G_4 = G_3$.

For automatic tuning of the designed filter, we have used a compact size piezomotor known as the tiny ultrasonic linear actuator [16]. This actuator can drive the tuning disks in both directions by switching the polarity of the applied ramp voltage. Travel distance of the actuator and also its speed is controlled by the number of pulses and the frequency of the applied signal, respectively. The operation of the piezomotor is explained in more detail in [17]. The piezomotors have been integrated on top of the lid of the tunable resonators without requiring significant additional space, as shown in Fig. 14. In this configuration, the moving part of the piezomotor is attached to a metallic bracket fixed on the lid and the shaft itself is connected to the tuning disk. As a result, it is the shaft and the tuning disk that can move forward and backward depending on the polarity of the pulses applied on the piezo driver.

The measured tuning performance of a single resonator with piezomotor is shown in Fig. 15. The center frequency is at 2.6 GHz and by changing the gap in the positive or negative direction (20-μm steps) it can be tuned from 2.565 to 2.635 GHz. Measured Q is from 2252 to 2914 over the tuning range. A six-pole tunable bandpass filter was assembled with piezomotors, as shown in Fig. 16. The measured S-parameters at $f_1 = 2.535$ GHz, $f_2 = 2.6$ GHz, and $f_3 = 2.635$ GHz are presented in Fig. 17. A tuning range of 70 MHz is achieved while the maximum insertion loss is less than 2.3 dB over the tuning range. The return loss is better than 16.2 dB for both ports and the required rejection level of 25 dB at 5-MHz offset from the passband is achieved for the designed filter.

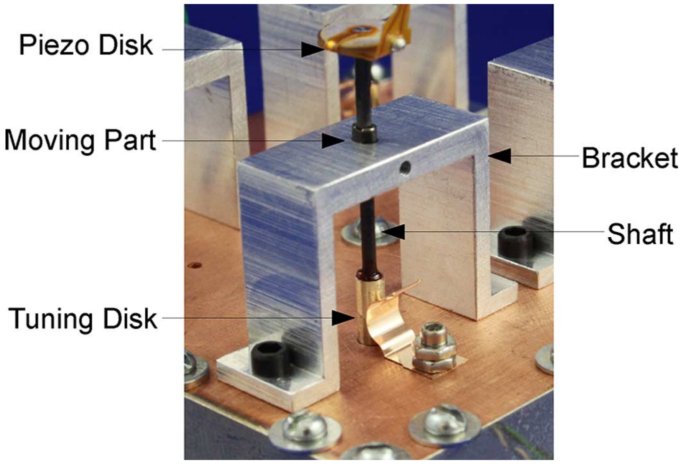

Fig. 14. Piezomotor assembled on top of the cavity resonator.

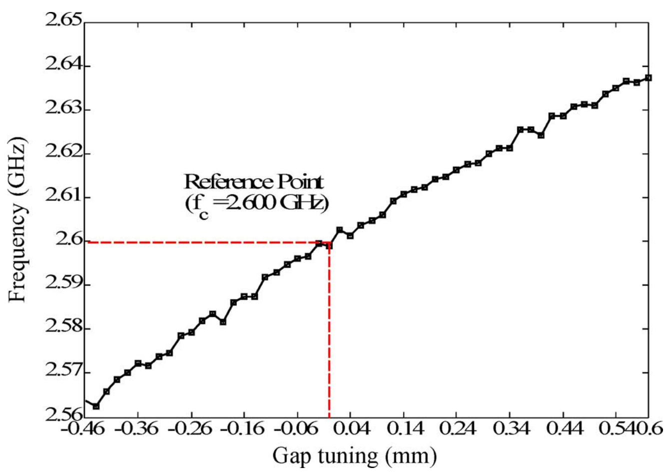

Fig. 15. Measured tuning performance for a single-cavity resonator using piezomotor with 20-μm step size.

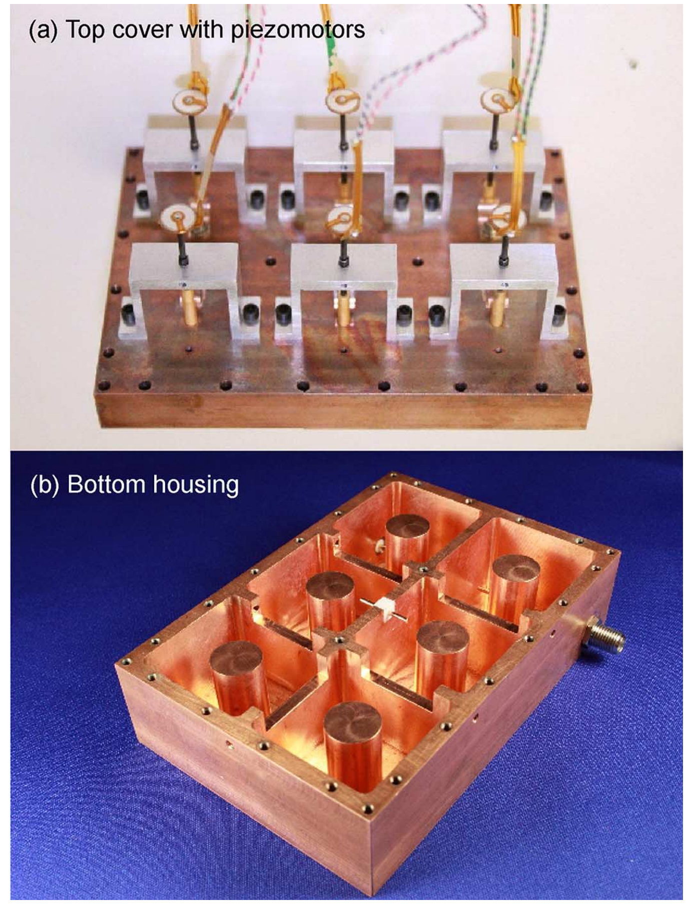

Fig. 16. Six-pole tunable bandpass filter with piezomotors.

B. Tunable WiMAX Filter With MEMS Capacitor Bank

In this section, a second six-pole tunable combline bandpass filter using RF-MEMS switched capacitor banks as tuning elements is presented. Using MEMS tuning circuits, it is possible to reduce the size, weight, and cost and also improve tuning speed compared to the mechanical tuning using piezomotors. The tuning speed of the filter with piezomotors is in the range of a few milliseconds depending on the required change in the gap values for tuning disks. Typical switching speed of the electrostatic RF-MEMS switches is in the range of a few tens of microseconds. The EM model of the filter is shown in Fig. 18 with the MEMS tuning circuits on top of the lid. The geometric dimensions of the filter are the same as the ones in Table II. For the MEMS tuning circuit, we have used the same capacitor bank as in Fig. 3 with different capacitance values; $C_1 = 0.2$ pF, $C_2 = 0.3$ pF, $C_3 = 0.5$ pF, and $C_4 = 0.7$ pF. Due to the symmetric structure of the six-pole filter, the capacitor banks for resonators R_1 and R_6 have the same values; $C_{\rm bank1} = C_{\rm bank6}$, and in the same way, $C_{\rm bank2} = C_{\rm bank5}$ and $C_{\rm bank3} = C_{\rm bank4}$. The final optimization of the EM model was performed with HFSS and for $C_{\rm bank1} = C_{\rm bank2} = C_{\rm bank3} = 0.7$ pF at $f_c = 2.6$ GHz. The only parameters that are optimized are the gap values for each resonator G_i $(i = 1, \ldots, 6)$. Fig. 19 shows the simulated S-parameters of the optimized filter at 2.6 GHz. After optimization at 2.6 GHz, the filter can be tuned only by adjusting the capacitance values of the capacitor banks on each resonator.

The six-pole tunable bandpass filter with MEMS capacitor banks is assembled as shown in Fig. 20. The tuning screws are used for initial tuning at 2.6 GHz and when $C_{\rm bank1} = C_{\rm bank2} = C_{\rm bank3} = 0.7$ pF. In order to maintain a high Q and low insertion loss for the assembled filter, it is very important to establish a good ground contact between the MEMS capacitor banks and the cavity wall. For this reason, grounding gaskets on the lid and also sufficient number of via-holes between the bottom ground plane of the PCB and the top ground plane of the MEMS capacitor bank are required, as shown in Fig. 20. The measured S-parameters of the filter at 2.6 GHz and after initial tuning are illustrated in Fig. 19. The maximum insertion loss is 2.5 dB and the return loss is better than 15 dB. The measured center frequency is 2.606 GHz and the bandwidth is 28 MHz. The tuning performance of the filter is presented in Fig. 21 when the value of the capacitor banks $C_{{\rm bank}i} (i = 1, \ldots, 6)$ is changed from 0 to 1.7 pF. A maximum tuning range from 2.634 to 2.590 GHz (44 MHz) is achieved while the insertion loss varies between 2.5–4.25 dB over the tuning range. As discussed in Section VI

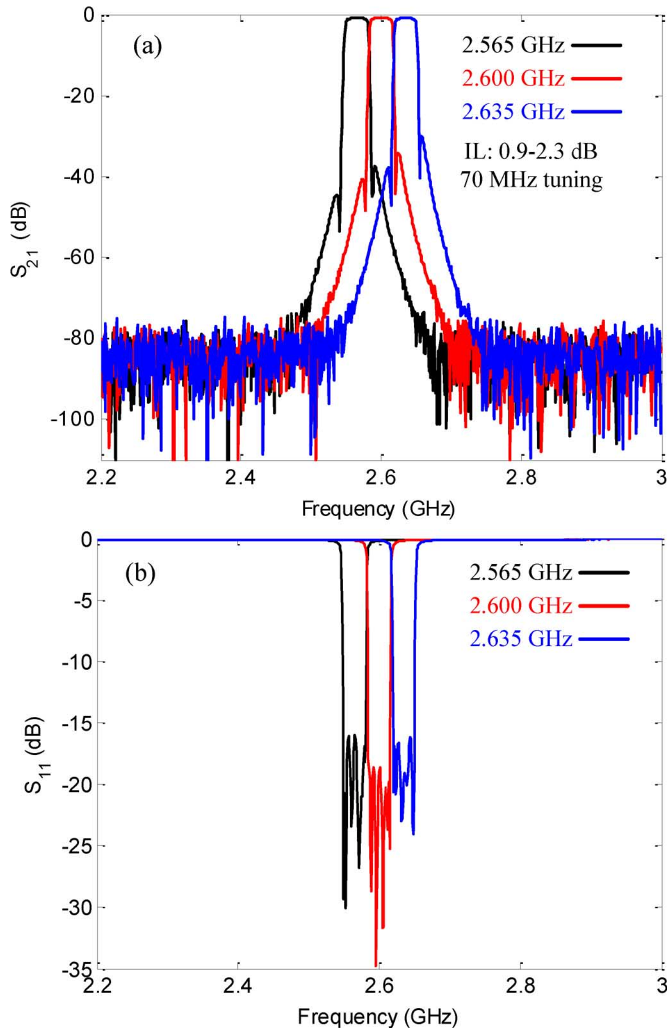

Fig. 17. Measured S-parameters of the tunable filter with piezomotors.

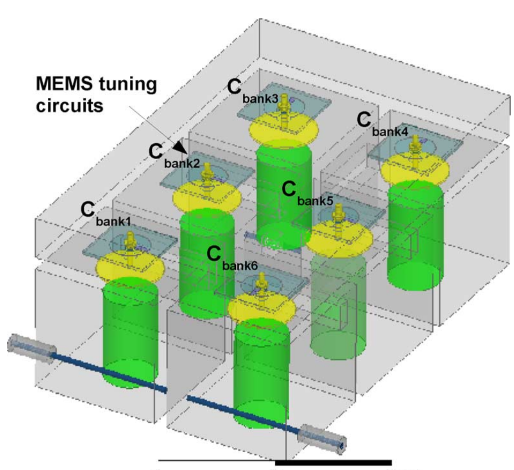

Fig. 18. 3-D EM model of the six-pole tunable bandpass filter with MEMS tuning circuits.

for this filter, all the capacitor banks are tuned to the same capacitance value (synchronous tuning), which results in the degradation of the return loss and also insertion loss over the tuning range.

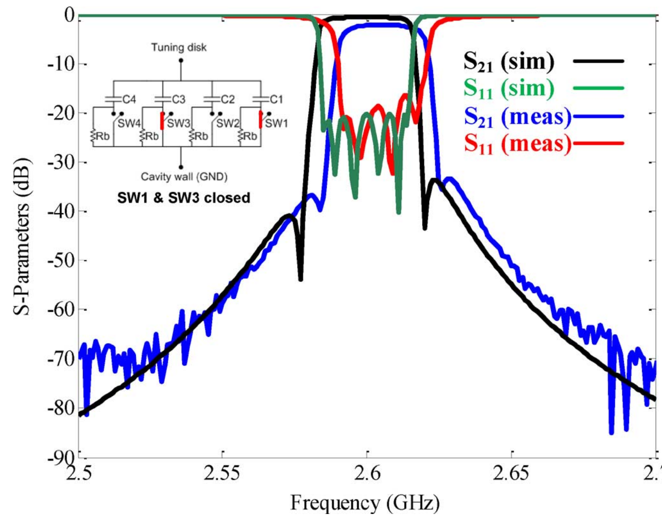

Fig. 19. Simulated and measured S-parameters of the optimized filter after initial tuning for $C_{\rm bank1} = C_{\rm bank2} = C_{\rm bank3} = 0.7$ pF at $f_c = 2.6$ GHz.

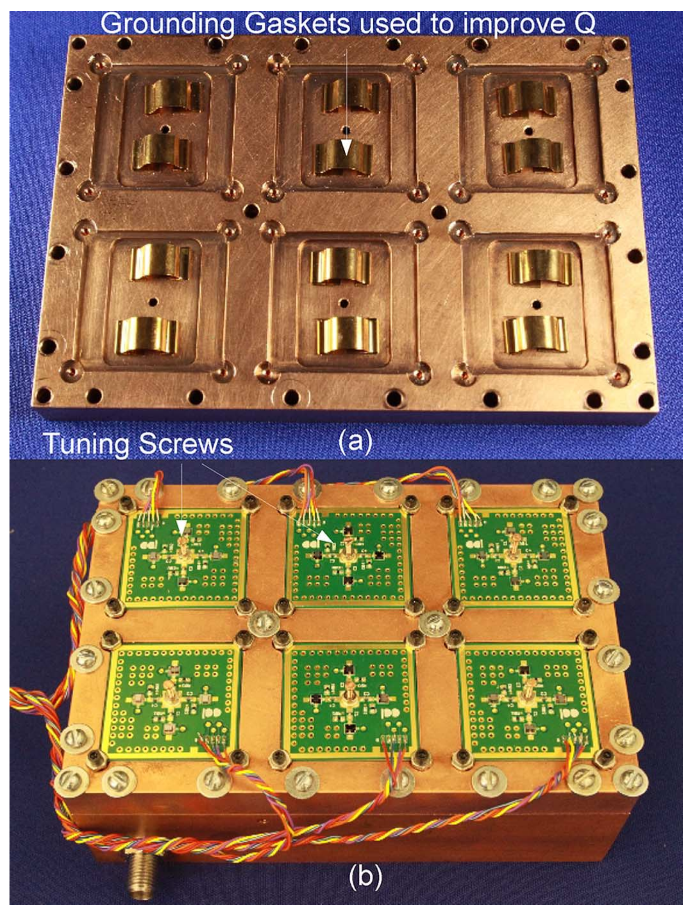

Fig. 20. Assembled six-pole tunable bandpass filter with MEMS capacitor banks.

VI. Discussion

Fig. 22 shows the narrowband measured tuning response of the six-pole tunable filter with MEMS capacitor banks. As shown in this figure, there is a degradation of the return loss (S_{11}) after tuning the center frequency from 2.6 GHz. This is due to the synchronous tuning of the resonators with the

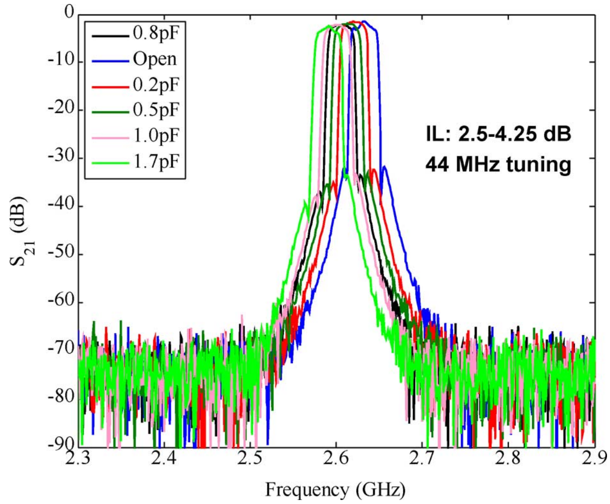

Fig. 21. Measured tuning performance of the filter for $C_{\rm bank} = 0 - 1.7$ pF.

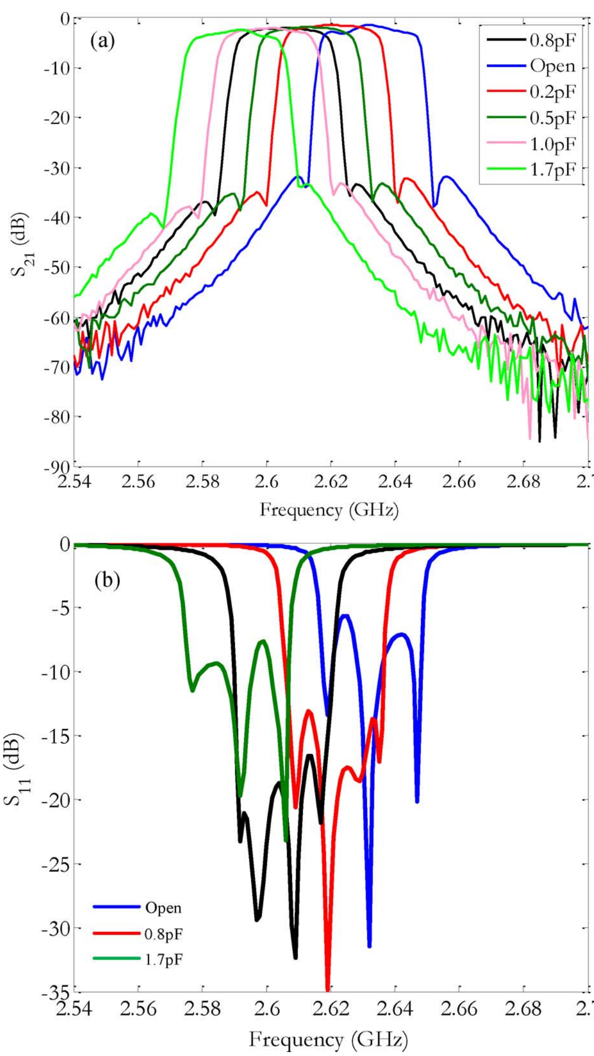

Fig. 22. Measured: (a) S_{21} and (b) S_{11} of the tunable filter with synchronous tuning of the resonators.

same value of capacitor banks ($C_{\rm bank1} = C_{\rm bank2} = C_{\rm bank3}$). For the two-pole filter described in Section IV, this is not an issue. However, for higher order tunable filters, it is necessary

TABLE III
REQUIRED CAPACITANCE VALUES FOR ASYNCHRONOUS TUNING

Frequency	$C_{bank1,6}$	$C_{bank2,5}$	$C_{bank3,4}$
2.565 GHz	1.14pF	1.24pF	1.19 pF
2.600 GHs	0.7pF	0.7pF	0.7pF
2.635 GHz	0.28pF	0.14pF	0.20pF

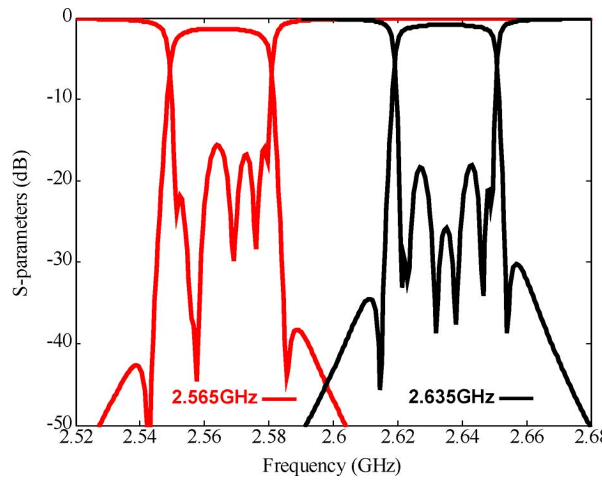

Fig. 23. Simulated S-parameters of the tunable filter with asynchronous tuning at extremes of the tuning range.

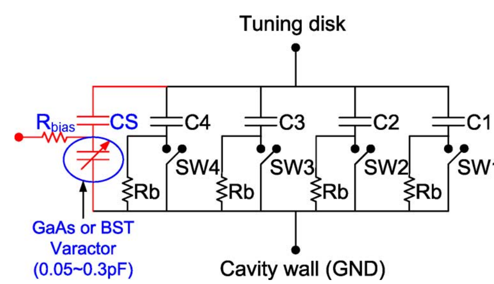

Fig. 24. Modified MEMS capacitor bank for asynchronous tuning.

to tune the resonators asynchronously in order to maintain the required return loss level. For asynchronous tuning of the proposed filter, it is required to have a capacitance value for each capacitor bank that is optimized at a specific center frequency. Table III summarizes the optimized capacitance values of each capacitor bank required for asynchronous tuning of the filter. The simulated tuning response of the filter using capacitance values in Table III is presented in Fig. 23. Using the MEMS switched capacitor bank of Fig. 3, only discrete capacitance values can be achieved, which may not be equal to the values in Table III; therefore, to improve the performance of the filter, it is required to employ MEMS capacitor banks with analog tuning capability. This can be achieved by using a modified tuning circuit as the one shown in Fig. 24 where a GaAs or barium–strontium–titanate (BST) varactor with a capacitance value of (0.05–0.3 pF) is added in parallel to the previous tuning circuit. However, using this circuit, Q value, power handling, and linearity of the proposed filter will be limited by the performance of the varactor. Another approach is to use integrated RF-MEMS switched capacitor banks with analog tuning capability such as the ones reported in [18] where all the capacitors and MEMS switches are fabricated on a single die and wire-bonding or PCBs are not required for the tuning circuits. In addition to asynchronous tuning, this will also further improve the Q and insertion loss of the filter. However, this requires a dedicated RF-MEMS fabrication process, which may not be commercially available.

VII. Conclusion

In this paper, a novel electronic tuning approach to design tunable evanescent mode combline filters has been presented. The tuning is based on the capacitive loading instead of mechanical movement of the tuning disk. The capacitive loading, and as a result, the center frequency, can be adjusted by using RF-MEMS switched capacitor banks. The use of commercially available SPST contact type RF-MEMS switches not only makes the tunable filter extremely compact, with near to zero dc power consumption and fast tuning speed, it also maintains a high-Q value of the filter over the entire tuning range by placing the tuning elements outside the cavity. Different filter prototypes were presented with two and six poles. The two-pole tunable filter achieves a tuning range of 110 MHz with a Q value higher than 374 (1300–374) over the entire tuning range. The six-pole filters were implemented using both MEMS tuning circuits and piezomotors. The tunable filter with piezomotors demonstrates superior RF performance with a 70-MHz tuning range, insertion loss less than 2.3 dB, and a rejection level better than 25 dB. The six-pole filter with MEMS tuning circuits achieves a tuning range of 44 MHz, while the insertion loss is better the 4.25 dB over the tuning range. To our knowledge, this is the first implementation of a tunable bandpass filter with an order higher than two using commercially available RF-MEMS tuning circuits. The performance of the proposed filters can be further improved by utilizing asynchronous tuning of the resonators and also by using integrated RF-MEMS switched capacitor banks.

References

[1] T. Shen, K. A. Zaki, and C. Wang, “Tunable dielectric resonators with dielectric tuning disks,” *IEEE Trans. Microw. Theory Techn.*, vol. 48, no. 12, pp. 2439–2445, Dec. 2000.

[2] S. W. Chen, K. A. Zaki, and R. G. West, “Tunable, temperature-compensated dielectric resonators and filters,” *IEEE Trans. Microw. Theory Techn.*, vol. 38, no. 8, pp. 1046–1052, 1990.

[3] J. Krupka, A. Abramowicz, and K. Derzakowski, “Magnetically tunable filters for cellular communication terminals,” *IEEE Trans. Microw. Theory Techn.*, vol. 54, no. 6, pp. 2329–2335, Jun. 2006.

[4] A. R. Brown and G. M. Rebeiz, “A varactor-tuned RF filter,” *IEEE Trans. Microw. Theory Techn.*, vol. 48, no. 7, pp. 1157–1160, Jul. 2000.

[5] B.-W. Kim and S.-W. Yun, “Varactor-tuned combline bandpass filter using step-impedance microstrip lines,” *IEEE Trans. Microw. Theory Techn.*, vol. 52, no. 4, pp. 1279–1283, Apr. 2004.

[6] M. A. El-Tanani and G. M. Rebeiz, “High-performance 1.5–2.5-GHz RF-MEMS tunable filters for wireless applications,” *IEEE Trans. Microw. Theory Techn.*, vol. 58, no. 6, pp. 1629–1637, Jun. 2010.

[7] S.-J. Park, K.-Y. Lee, and G. M. Rebeiz, “Low-loss 5.15–5.70-GHz RF MEMS switchable filter for wireless LAN applications,” *IEEE Trans. Microw. Theory Techn.*, vol. 54, no. 11, pp. 3931–3939, Nov. 2006.

[8] C.-C. Cheng; and G. M. Rebeiz, “High-Q 4–6-GHz suspended stripline RF MEMS tunable filter with bandwidth control,” *IEEE Trans. Microw. Theory Techn.*, vol. 59, no. 10, pp. 2469–2476, Oct. 2011.

[9] S.-J. Park, I. Reines, C. Patel, and G. M. Rebeiz, “High-Q RF-MEMS 4–6-GHz tunable evanescent-mode cavity filter,” *IEEE Trans. Microw. Theory Techn.*, vol. 58, no. 2, pp. 381–389, Feb. 2010.

[10] H. Fengxi, S. Fouladi, and R. R. Mansour, “High-Q tunable dielectric resonator filters using MEMS technology,” *IEEE Trans. Microw. Theory Techn.*, vol. 59, no. 12, pp. 3401–3409, Dec. 2011.

[11] X. Liu, L. P. B. Katehi, W. J. Chappell, and D. Peroulis, “High-Q tunable microwave cavity resonators and filters using SOI-based RF MEMS tuners,” *J. Microelectromech. Syst.*, vol. 19, no. 4, pp. 774–784, Aug. 2010.

[12] K. Entesari, K. Obeidat, A. R. Brown, and G. M. Rebeiz, “A 25–75-MHz RF MEMS tunable filter,” *IEEE Trans. Microw. Theory Techn.*, vol. 55, no. 11, pp. 2399–2405, Nov. 2007.

[13] V. Sekar, M. Armendariz, and K. Entesari, “A 1.2–1.6-GHz substrate-integrated-waveguide RF MEMS tunable filter,” *IEEE Trans. Microw. Theory Techn.*, vol. 59, no. 4, pp. 866–876, Apr. 2011.

[14] S. Fouladi, F. Huang, W. D. Yan, and R. R. Mansour, “Combline tunable bandpass filter using RF-MEMS switched capacitor bank,” in *IEEE MTT-S Int. Microw. Symp. Dig.*, Jun. 2012.

[15] R. J. Cmeron, R. Mansour, and C. M. Kudsia, *Microwave Filters for Communication Systems: Fundamentals, Design and Applications*. New York: Wiley, 2007.

[16] “Piezoelectric ultrasonic motors,” Micromech. Inc., State College, PA, 2010. [Online]. Available: http://mmech.com/ultrasonic-motors/linear-motors

[17] J. A. Ruiz-Cruz, M. M. Fahmi, S. A. Fouladi, and R. R. Mansour, “Waveguide antenna feeders with integrated reconfigurable dual circular polarization,” *IEEE Trans. Microw. Theory Techn.*, vol. 59, no. 12, pp. 3365–3374, Dec. 2011.

[18] A. Grichener and G. M. Rebeiz, “High-reliability RF-MEMS switched capacitors with digital and analog tuning characteristics,” *IEEE Trans. Microw. Theory Techn.*, vol. 58, no. 10, pp. 2692–2701, Oct. 2010.

Siamak Fouladi (S’03–M’10) received the B.Sc. degree in electrical engineering from the University of Tehran, Tehran, Iran, in 2002, and the M.Sc. degree in electrical engineering from Concordia University, Montreal, QC, Canada, in 2005, and the Ph.D. degree in electrical engineering from the University of Waterloo, Waterloo, ON, Canada, in 2010.

In May 2005, he joined the Center for Integrated RF Engineering, University of Waterloo. He is currently a Research and Development Engineer with the Wireless Semiconductor Division (WSD), Avago Technologies, San Jose, CA. His research interests include RF-MEMS device fabrication and characterization, acoustic wave devices, and integrated millimeter-wave circuits.

Dr. Fouladi was the recipient of the Natural Sciences and Engineering Research Council of Canada (NSERC) Doctoral Award.

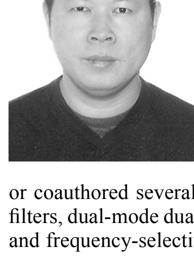

Fengxi Huang (S’11) received the B.Sc. degree in system engineering from the Nanjing University of Science and Technology, Nanjing, China, in 1998, the M.Sc. degree in mobile communication networks from the University of Kent, Canterbury, Kent, U.K., in 2006, and the Ph.D. degree in electrical engineering from the University of Waterloo, Waterloo, ON, Canada, in 2012.

He is currently a Research Scientist with the Center for Integrated RF Engineering (CIRFE), University of Waterloo, Waterloo. He has authored or coauthored several scientific papers. His research interests include tunable filters, dual-mode dual-band filters, diplexers, triplexers, transceivers, antennas, and frequency-selective surface design.

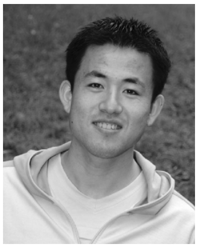

Winter Dong Yan (S'04–M'07) received the B.Sc. degree in automatic control from the Beijing Institute of Technology, Beijing, China, in 2000, and the M.Sc. degree in mechanical engineering and Ph.D. degree in electrical engineering from the University of Waterloo, Waterloo, ON, Canada, in 2002 and 2007, respectively.

Since 2007, he has been working within the wireless industry. He is currently with the Research and Development Center, Huawei Technologies, Kanata, Canada. He has authored or coauthored several publications in the area of RF passive component development for mobile devices. His current research interest includes MEMS technology and 3-D packaging technology for wireless applications.

Raafat R. Mansour (S'84–M'86–SM'90–F'01) was born in Cairo, Egypt, on March 31, 1955. He received the B.Sc. (with honors) and M.Sc. degrees in electrical engineering from Ain Shams University, Cairo, Egypt, in 1977 and 1981, respectively, and the Ph.D. degree in electrical engineering from the University of Waterloo, Waterloo, ON, Canada, in 1986.

In 1981, he was a Research Fellow with the Laboratoire de Electromagnetisme, Institut National Polytechnique, Grenoble, France. From 1983 to 1986, he was a Research and Teaching Assistant with the Department of Electrical Engineering, University of Waterloo. In 1986, he joined COM DEV Ltd., Cambridge, ON, Canada, where he held several technical and management positions with the Corporate Research and Development Department, becoming a Scientist in 1998. Since January 2000, he has been a Professor with the Electrical and Computer Engineering Department, University of Waterloo, where he was a Natural Sciences and Engineering Research Council of Canada (NSERC) Industrial Research Chair from 2001 to 2010. He currently holds a Canada Research Chair. He is the Founding Director of the Centre for Integrated RF Engineering. He has authored or coauthored numerous publications in the areas of filters and multiplexers, high-temperature superconductivity, and microelectromechanical systems (MEMS). He coauthored *Microwave Filters for Communication Systems* (Wiley, 2007). He holds several patents related to the areas of dielectric resonator filters, superconductivity and MEMS devices. His current research interests include MEMS technology and miniature tunable RF filters for wireless and satellite applications.

Dr. Mansour is a Fellow of the Engineering Institute of Canada (EIC) and the Canadian Academy of Engineering (CAE).